

MEASUREMENT OF VISIBLE AND UV EMISSIONS FROM
ENERGETIC NEUTRAL ATOM PRECIPITATION, (ENAP)

UNIVERSITY OF TEXAS AT DALLAS

PRINCIPAL INVESTIGATOR: BRIAN A. TINSLEY

CO INVESTIGATORS: W.B. HANSON

R.P. ROHRBAUGH

UTAH STATE UNIVERSITY

CO INVESTIGATOR: M.R. TORR

INSTRUMENT

IMAGING SPECTROMETRIC OBSERVATORY, BUILT BY MARSHA TORR, UTAH
STATE UNIVERSITY

INTERACTIONS OF PRECIPITATING ATOMS WITH THERMOSPHERE

IONIZATION

EXCITATION AND OPTICAL EMISSION

MOMENTUM TRANSFER (HEATING AND VIBRATIONAL EXCITATION)

SOURCES OF PRECIPITATING NEUTRALS

CHARGE EXCHANGE OF PLASMASPHERIC IONS AND EXOSPHERIC H AND O,

CHARGE EXCHANGE OF SOLAR WIND IONS WITH EXOSPHERIC AND INTER-
PLANETARY HYDROGEN

This figure, which is a print from S-201 frame 40 of a 1-min exposure centered on the earth, wavelength range 1050-1600 Å, was not available in a reproducible form for this document. It may be found in Apollo 16 Preliminary Science Report, NASA SP-315, November 1972, p. 13-8.

Figure 2

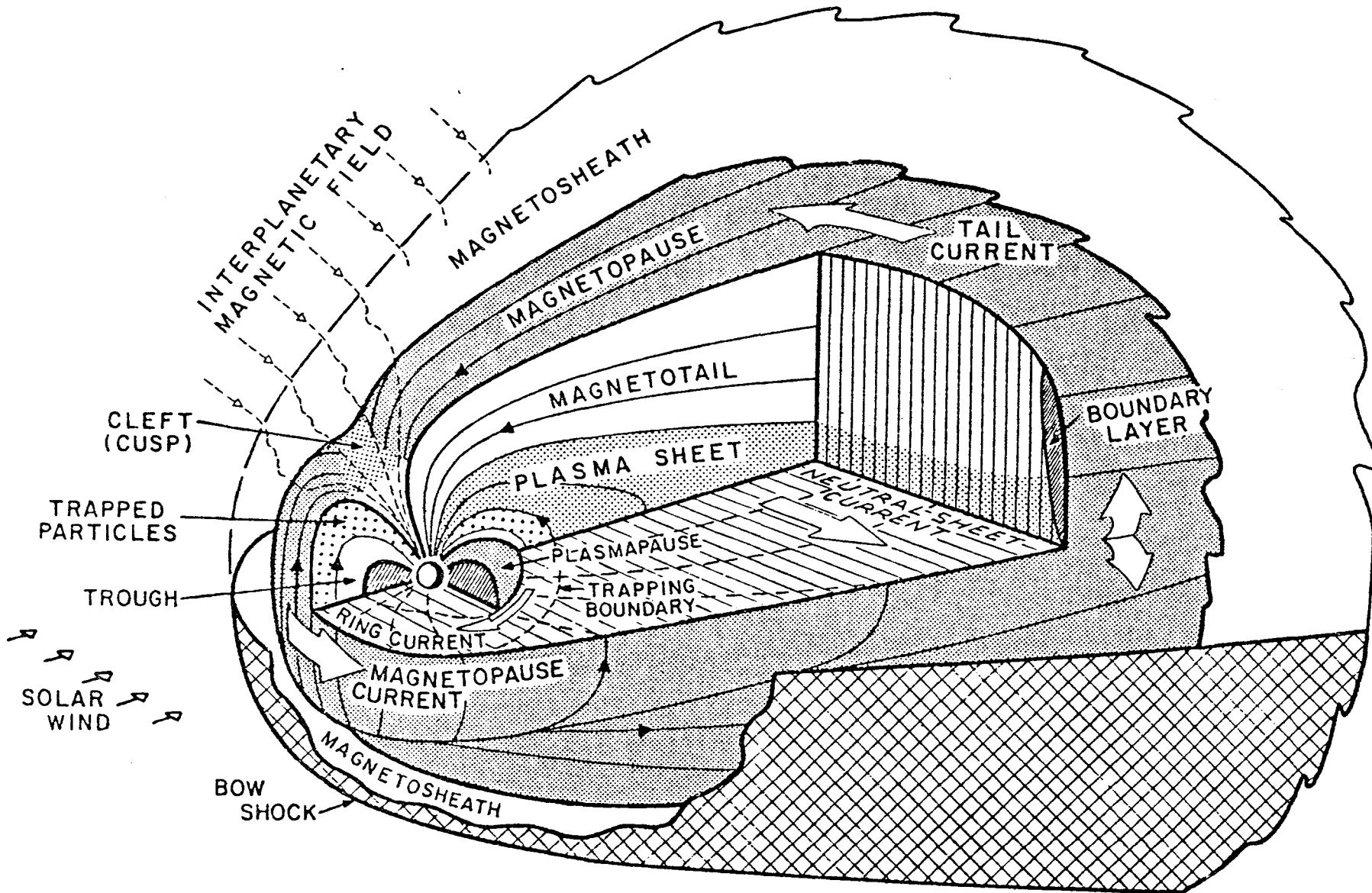
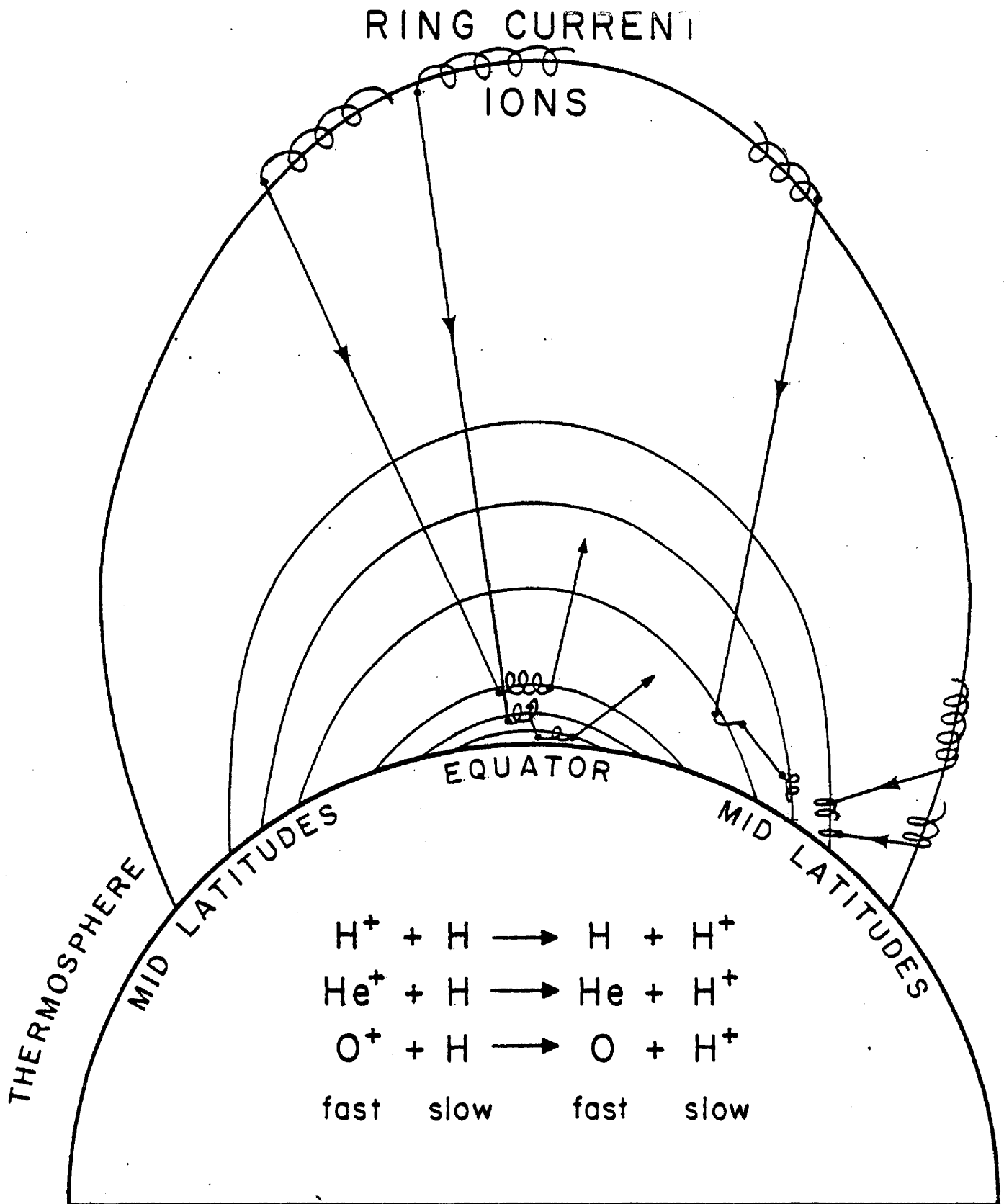


Figure 3

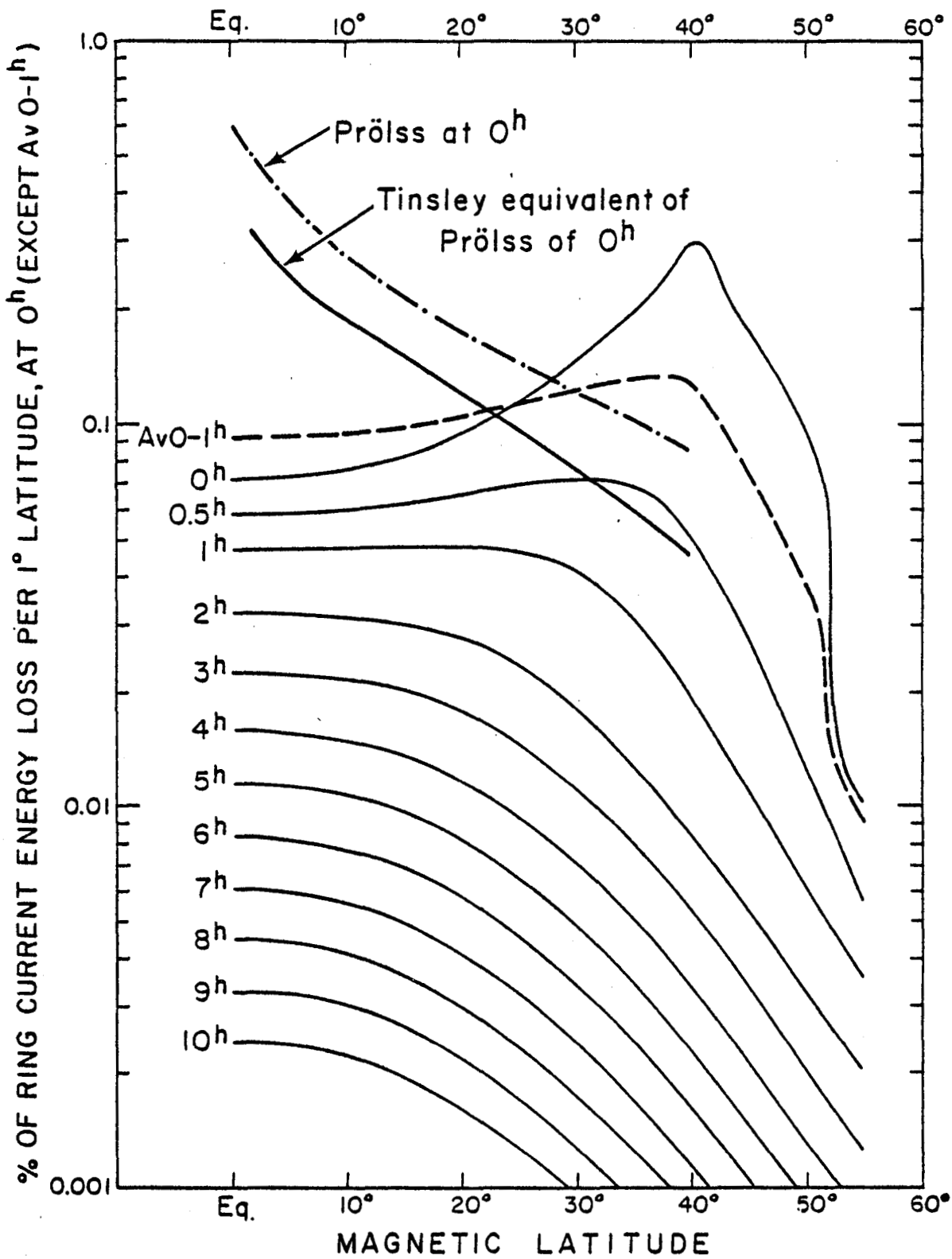


**POLAR SECTION
THROUGH MAGNETOSPHERE**

neutrals impacting the thermosphere. The trajectory of a neutral produced by charge exchange is determined by the direction the ion was moving at the instant of charge exchange - and for energies above a few ev the atoms travel in essentially straight lines. For isotropic ion velocity distributions there will be an isotropic production of neutrals, and most will escape the earth, with less than 10% impacting the thermosphere.

An important feature of the precipitation is that near the magnetic equator atoms moving nearly perpendicular to the magnetic field can become trapped again on their first ionizing collision (for some species and energies the probability of this happening is very low) and a low altitude belt of temporarily trapped ions is set up. Its energy spectrum is approximately that of the high altitude ring current, and its flux tends to rise and fall as the ring current flux changes. These particles go through a succession of charge exchange neutralization and ionization cycles, diffusing vertically in the process, before losing their energy. Such equatorial fluxes of trapped ions have been detected from satellites a number of times.

The latitude distribution of the precipitating neutrals has been calculated and is shown in Figure 5. These calculations are for a population of ions which are initially isotropic and on the L shell defined by $L = 3$ such as the isotropic distributions found where the ring current is interacting with the plasmasphere at the plasmopause. As the ions are lost by charge exchange those which mirror at lowest altitudes are lost fastest (the exospheric hydrogen has a scale height of about 1000 km). Thus the ions with equatorial pitch angles nearest to 0° or 180° are lost fastest, and the pitch angle distribution evolves with time toward a pancake distribution, and the latitude distribution shrinks towards the equator. For a distribution composed of 90°



ISOTROPIC PITCH ANGLE DISTRIBUTION ON L SHELL = 3 AT 0^h

Figure 5

equatorial pitch angle particles, all motion would be confined to the equatorial plane, and all particles would be precipitated essentially at the magnetic equator. The timescale for this figure corresponds to 1-30 keV H^+ ions in the ring current with exospheric hydrogen concentration and altitude distribution for a 950°K exospheric temperature. For other species the charge exchange cross sections are smaller, hence the time scale is longer. Figure 6 shows the variation of reaction rate σv (inversely proportional to lifetime) for several ring current species. Figure 7 shows the latitude distribution of precipitating neutrals for isotropic pitch angle distributions on various L-shells shown. There is a peak influx rate of about 15° equatorward at the foot of the L-shell on which the ring current ions are located. This is particularly interesting since SAR-arcs are found 10-15° inside the latitude of the hydrogen auroral arcs that result from directly precipitating ring current protons. While precipitating neutrals probably don't directly excite easily detectable optical emissions, or the strong 6300 Å emission of SAR-arcs (hot electrons seem to be the cause of that), the precipitating neutrals might heat the atmosphere sufficiently that F-region composition is enhanced in molecular constituents and might also vibrationally excite the molecules, so that dissociative recombination is accelerated, producing the electron density troughs observed. In such low electron density regions the downward conduction by electrons of ring current energy will heat the ionospheric electrons sufficiently to excite 6300 emission.

Most plasmaspheric ions do not have isotropic distributions, however, and for ions at low L values that have been radially transported inward by transverse electric fields, and which have been subject to erosion by charge

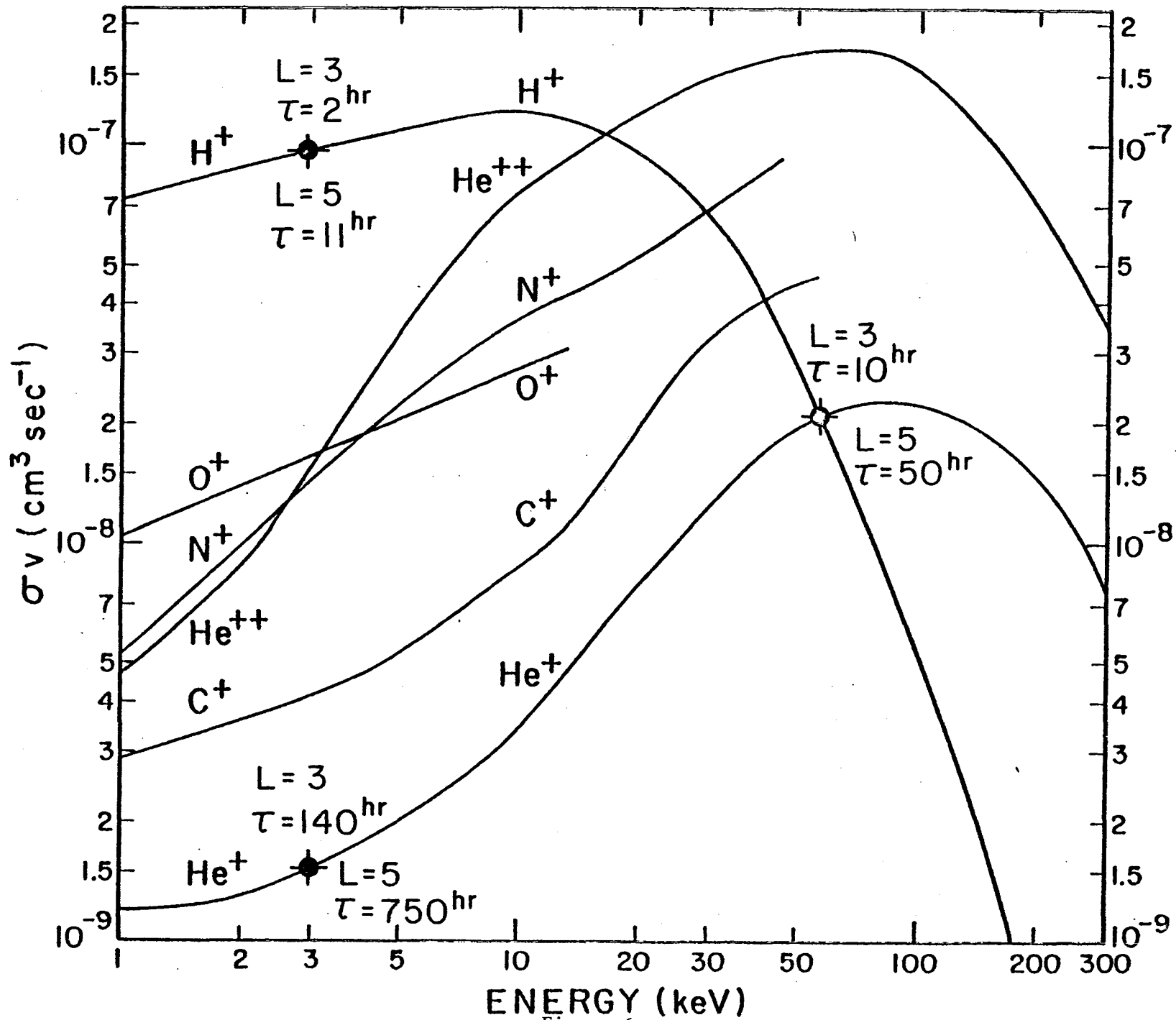
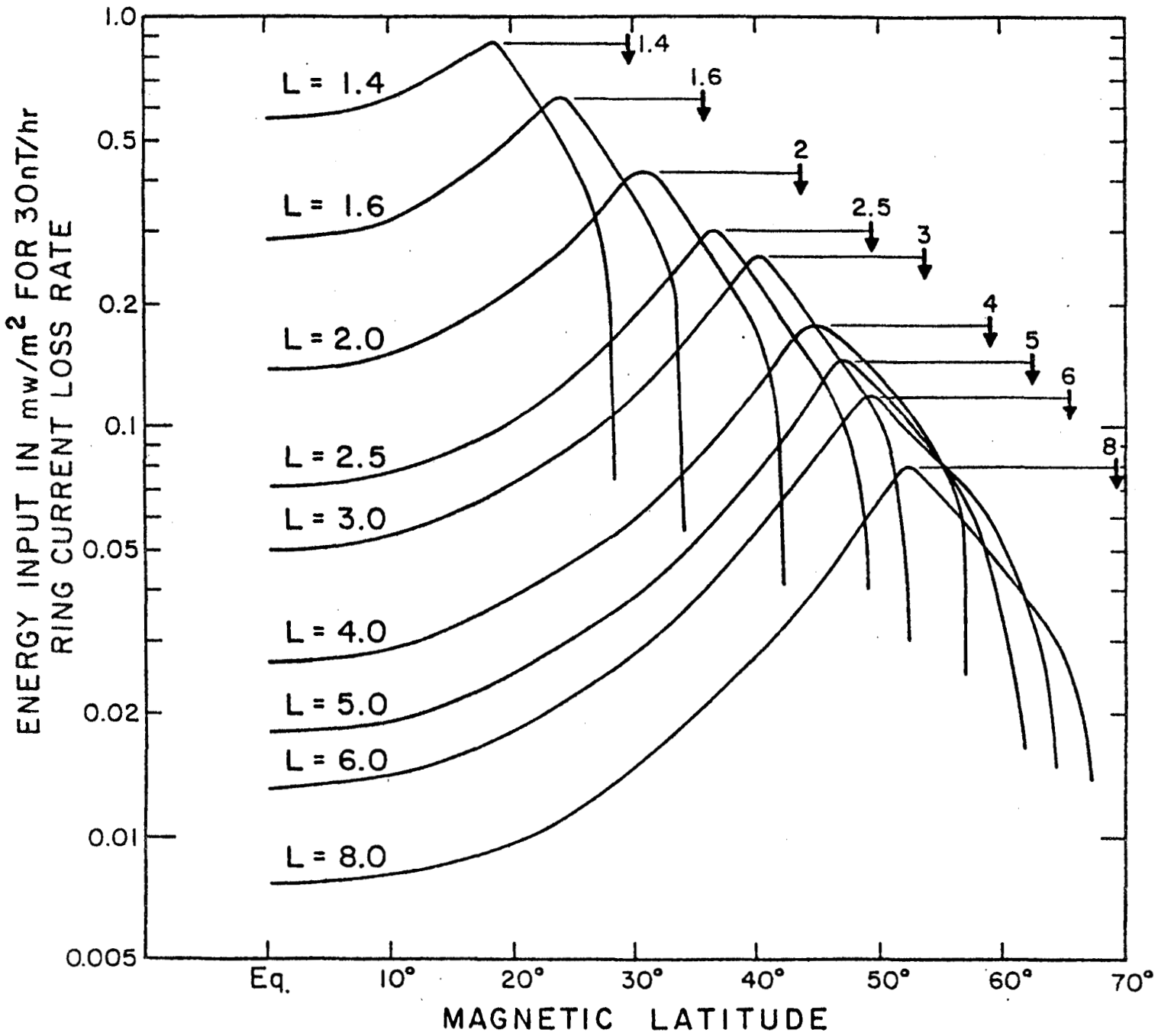


Figure 6



LATITUDE VARIATION OF ENERGETIC NEUTRAL INFLUX FOR ISOTROPIC PITCH ANGLE DISTRIBUTION ON SHELLS OF L-VALUE LISTED THE ARROW MARKS LATITUDE OF FOOT OF L-SHELL

Figure 7

exchange for days or weeks, a very highly anisotropic pancake pitch angle distribution is found. It is apparently a combination of this anisotropic source, together with an increased efficiency of trapping at low altitudes, which results in the equatorial low altitude trapped particles. Fig. 8 shows the latitude variation of several thermospheric manifestations of neutral atom precipitation. The histogram is trapped protons from precipitating MeV H atoms, according to Hovestadt; the smooth curve is $\text{He}^+ 304 \text{ \AA}$ emission from precipitating MeV helium, according to Meier, and the sawtooth curve is the latitude variation of 'probability of occurrence' of H Balmer α emission from precipitating H atoms, according to Levasseur.

With the spacelab observations, we expect to be able to see very faint emissions, of order 10^{-1} to $10^{-2} R$, with time integration, and thus to see the effects of neutral atom precipitation in quiet as well as disturbed times. We will look for emissions not previously detected, and one very important objective is to identify the precipitation of atomic oxygen. We will look for oxygen emissions of higher excitation potential than those produced by recombination, and we will look for lines of hydrogen and helium at low altitudes of intensity greater than that possible from resonant scattering, and for all three for lines of doppler widths greater than could be produced by resonant scattering or chemical excitation. One characteristic of collisional excitation by heavy particles is that they transfer momentum and excite vibrational levels of molecules, thus high vibrational excitation of N_2^+ IRG emissions is a signature of hydrogen atoms or protons below 2 keV, of helium ions or atoms below 8 keV, or oxygen atoms or ions below 30 keV.

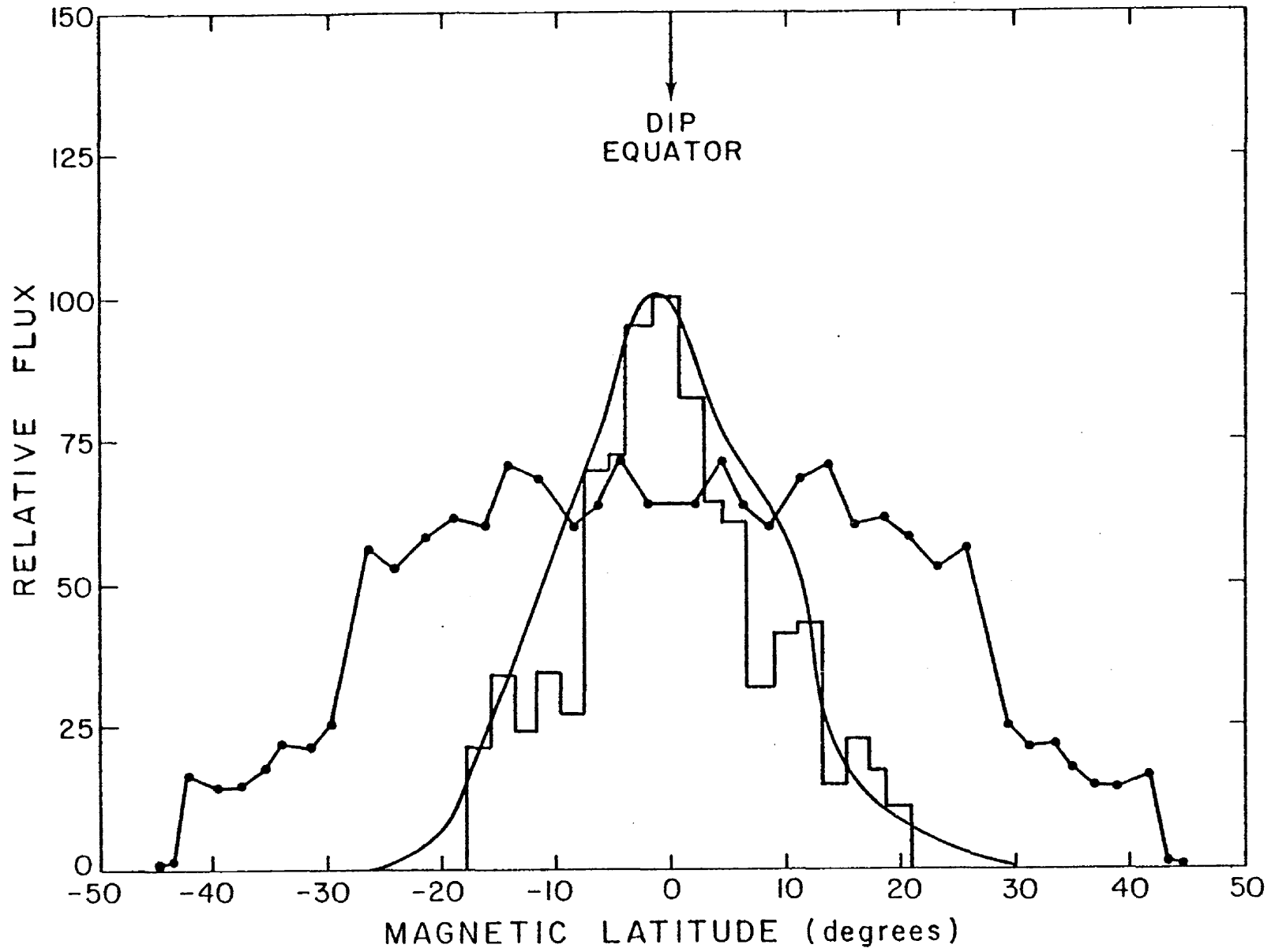


Figure 8

We will be using special techniques to detect the presence of faint lines in the presence of background emissions, such as the zodiacal light and background starlight. One is to minimize the background by selecting viewing directions at high galactic and ecliptic latitudes. This will be somewhat constrained by the need to imaging the limb for altitude profiles of the emissions. However, whatever astronomical backgrounds are present will be viewed at high zenith angles on a different part of the orbit, and subtracted later. Non astronomical backgrounds would be mainly recombination emissions, and as noted earlier, the particle precipitation emissions are distinguishable on the basis of different doppler widths, and different vibrational ratios for molecular emissions.

I am sure that part of the background we will be identifying and subtracting will be emissions due to the artificial environment introduced by the shuttle, and excited by active experiments on the shuttle, so we hope to be of use to other experiments in providing data on these too. The final figure summarizes the functional objectives.

FUNCTIONAL OBJECTIVES OF ENAP

1. EVALUATE RELATIVE FLUXES OF DIFFERENT SPECIES INVOLVED IN NEUTRAL ATOM PRECIPITATION BY MEASURING INTENSITIES OF SPECIFIC EMISSIONS.
2. EVALUATE ENERGY SPECTRUM OF PRECIPITATING NEUTRALS BY MEASURING (A) DOPPLER PROFILES (B) VIBRATIONAL RATIOS (C) ALTITUDE PROFILES FROM LIMB SCANNING OF EMISSIONS.
3. EVALUATE LATITUDE DISTRIBUTION OF PRECIPITATION BY MAKING OBSERVATIONS OVER A RANGE OF LATITUDES, IN FACT THE COMPLETE LATITUDE RANGE DEFINED BY THE ORBIT OF SPACELAB.
4. EVALUATE THE TIME VARIATION OF THE FLUXES OF PRECIPITATING NEUTRALS, AND OF THE LATITUDE DISTRIBUTIONS, PARTICULARLY AS IT IS RELATED TO VARIATIONS IN Dst AND K_p . FOR THIS THE MORE TIME SPENT IN NIGHTTIME OBSERVATION, UP TO THE MAXIMUM DURATION OF THE MISSION, THE BETTER THE SCIENTIFIC RETURN.
5. EVALUATE THE EFFECTS ON THE ATMOSPHERE, PARTICULARLY HEATING, VIBRATIONAL EXCITATION AND PRODUCTION OF IONIZATION, BY OPTICAL OBSERVATIONS AND IF POSSIBLE OTHER SPACELAB. SATELLITE AND GROUND BASED OBSERVATIONS, AND COMPARE WITH EFFECTS CALCULATED FROM EVALUATED FLUXES.
6. EVALUATE THE EFFECTS OF LOSS OF RING CURRENT IONS OF SPECIFIC ENERGIES, SPECIES, AND PITCH ANGLES ON THE EVOLUTION OF THE RING CURRENT, AND COMPARE WITH OTHER SATELLITE AND GROUND BASED (MAGNETIC) OBSERVATIONS.

Figure 9

SECTION V. WIDE ANGLE MICHELSON DOPPLER
IMAGING INTERFEROMETER (WAMDII)

